EDGE ENHANCEMENT OF INFRARED IMAGERY BY WAY OF THE ANISOTROPIC DIFFUSION PYRAMID

Scott T. Acton

The Oklahoma Imaging Laboratory
School of Electrical and Computer Engineering, Oklahoma State University
Stillwater, Oklahoma 74078
sacton@taco.ecen.okstate.edu

ABSTRACT

The problem of enhancing and detecting edges in infrared images is addressed in this paper. The proposed solution utilizes a multiresolution structure called the anisotropic diffusion pyramid (ADP), which is created by successive application of anisotropic diffusion and subsampling. A pyramid node linking process is used to segment the image and to detect edges. For the slowly varying sigmoidal edges in the IR imagery, it is shown that the diffusion process is effective in edge enhancement. Furthermore, system parameters are derived to maximize the edge sharpening ability of the ADP. The ADP avoids the "staircase" artifacts of single-resolution diffusion algorithms and avoids the localization and region merging problems of pyramids based on linear filters.

1. BACKGROUND

To detect edges and segment images in real-time applications such as infrared (IR) search and track, multiresolution approaches have been applied because of their computational efficiency. Image pyramids may be used to achieve exponential improvements in computational expense [1]. The traditional pyramidal structure employed is the Gaussian pyramid, which contains a family of images that have been successively smoothed using a linear Gaussian-weighted filter and subsampled [1]. The linear, isotropic smoothing of the Gaussian pyramid leads to region merging and edge localization problems that increase with each level of the pyramid. When applied to the already dull edges of the IR images, the Gaussian pyramid is ineffective in accurately detecting image region boundaries.

Here, the adaptive smoothing of anisotropic diffusion is used in a pyramidal framework [2]. Anisotropic diffusion encourages intra-region smoothing over inter-region smoothing and enhances edges [3]. On a continuous surface, the diffusion equation for the intensity at location (x,y) of an image I at time t is given by

$$I_t(x,y) = \mathrm{div}\left[c_t(x,y)\nabla I_t(x,y)\right] \tag{1}$$

This work is supported by the U.S. Army Research Office.

where ∇ is the gradient operator, div is the divergence operator, and $c_t(x,y)$ is the diffusion coefficient. $c_t(x,y)$ remains constant for all (i,j) in isotropic diffusion, and is allowed to vary according to the magnitude of the local image gradient in anisotropic diffusion. One possible realization of the diffusion coefficient is

$$c_t(x,y) = \exp\left\{-\left[\frac{\nabla I_t(x,y)}{k}\right]^2\right\} \tag{2}$$

where k controls the feature scale retained. A method for selecting k is discussed in this paper.

For digital imagery, a discrete version of the diffusion equation is given in [3] as follows:

$$I_{t+1}(x,y) = I_t(x,y) + (1/4)\begin{bmatrix} c_{N,t}(x,y)\nabla I_{N,t}(x,y) + c_{S,t}(x,y)\nabla I_{S,t}(x,y) \\ +c_{E,t}(x,y)\nabla I_{E,t}(x,y) + c_{W,t}(x,y)\nabla I_{W,t}(x,y) \end{bmatrix} \tag{3}$$

The four diffusion coefficients and four gradients in (3) correspond to the four directions (north, south, east, and west) w.r.t. the location (x,y). Each coefficient and gradient is computed in the same manner. For example, the coefficient for diffusion in the northern direction is

$$c_{N,t}(x,y) = \exp\frac{-\nabla I_{N,t}^2(x,y)}{k^2} \tag{4}$$

where $\nabla I_{N,t}(x,y) = I_t(x,y+1) - I_t(x,y)$.

Now, the diffusion operation can be combined with the sampling operation to create an anisotropic diffusion pyramid (ADP). The ADP for an NxN image contains a maximum of $\log_S N + 1$ levels if 1 of S sampling is applied to each image row and column to produce the next pyramid level. The base, level 0, is the original image, and level R (where $1 \le R \le \log_S N$) is the selected *root level* for segmentation. Each node of the original image is linked to a node of the root level. So, higher values of R will yield a coarse edge map with fewer image regions. With each ascending level in the pyramid, diffusion is enacted and the results are subsampled to produce the next pyramid level. Node positions in the pyramid are denoted by the position

0-7803-3258-X/96/$5.00 © 1996 IEEE

(x,y) and the pyramid level l. The node values $P_l(x,y)$ are initialized as follows:

$$P_{l+1}(x,y) = P_l(2x,2y) + (1/4)\begin{bmatrix} c_{N,l}(2x,2y)\nabla I_{N,l}(2x,2y) + c_{S,l}(2x,2y)\nabla I_{S,l}(2x,2y) \\ +c_{E,l}(2x,2y)\nabla I_{E,l}(2x,2y) + c_{W,l}(2x,2y)\nabla I_{W,l}(2x,2y) \end{bmatrix} \quad (5)$$

where the diffusion coefficients and gradients are computed as in (3), using the node values from level l in the neighborhood of $(2x,2y)$. Construction of the entire ADP is less expensive computationally than performing one iteration of diffusion on one third of the original image.

After the pyramid node values are computed from level 0 to the root level R, multiresolution segmentation and edge detection are accomplished using pyramid node linking. The linking process actually consists of two basic steps: linking and propagating root values to the base. In the linking stage, node values on each level are linked to the parent node in the next highest level that is most similar in image intensity. For our implementation, each node is linked to one of S^2 possible parents. Linking starts at the pyramid base and proceeds to level R - 1. Once linking is completed, the root values are propagated to each base pixel and edge detection is performed at the original resolution, but using the associated root values to locate discontinuities. The pyramidal edge detection process is resilient to noise, clutter, and spurious detail. With this approach, the typically heuristic thresholding process is eliminated from edge detection.

2. ANALYSIS

Pyramidal segmentation approaches that involve linear filtering are particularly troublesome for IR imagery, as the filtering process blurs the already "dull" edges. To improve edge localization for edge-based applications, anisotropic diffusion is utilized. Nevertheless, anisotropic diffusion does have drawbacks. One major limitation for IR imagery is the so-called "staircasing" effect. With a slowly increasing (or decreasing) edge, several erroneous plateaus may be created in the diffusion process and may be interpreted incorrectly as intermediate surfaces [4]. Using the anisotropic diffusion pyramid (ADP), the edge localization and edge sharpening properties of anisotropic diffusion can be exploited, while, at the same time, the edge detector performance is improved by a multiresolution hierarchical process.

In this section, a 1-D model of an infrared edge is given. The edge model is used to exhibit the edge enhancement ability of the ADP. Also, the model is applied in order to determine the value of k for use in (5) that maximizes the edge sharpening. Additionally, the root level R is determined that leads to step edges in the enhanced imagery.

The sigmoidal edges found in the IR imagery may be modeled in 1-D by

$$I_t(x) = A\tanh(fx+\theta) + B \quad (6)$$

where A is the magnitude of the edge, f dictates the edge rate of change, θ is the edge phase (displacement), and B is the baseline value of the edge. This function will have a maximum value of $B + |A|$ and a minimum value of $B - |A|$. The inflection point (the center) of the edge is at $x_{ip} = -\theta/f$. The slope at the inflection point is Af. As f is increased, the edge approaches a step edge. An example plot of the sigmoidal edge model is given in Fig. 1.

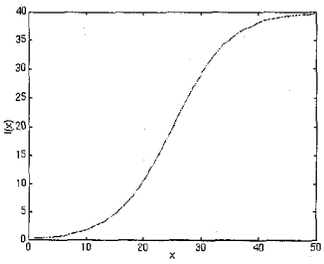

Fig. 1: The sigmoidal edge model for A = 20, B = 20, f = 0.1, and θ = -2.5.

Perona and Malik [3] gave the following 1-D (continuous) version of the diffusion equation:

$$I_t(x) = \frac{\partial}{\partial x}\phi(I_t(x)) = \phi'(I_t(x))\cdot I_t''(x) \quad (7)$$

where $\phi(I_t(x))$ is the flux function and is given by $\phi(I_t(x)) = c_t(x)I_t'(x)$. To evaluate how anisotropic diffusion enhances the edges of the IR imagery, the slope of the edge must be examined w.r.t. time. Perona and Malik provided a method to compute $\frac{\partial}{\partial t}[I_t'(x)]$ by changing the order of differentiation (given a continuously differentiable diffusion coefficient):

$$\frac{\partial}{\partial t}[I_t'(x)] = \phi''\left[I_t''(x)\right]^2 + \phi' I_t'''(x) \quad (8)$$

It is shown in [3] that $I_t'(x)$ will always be increasing in the neighborhood of x_{ip}, so that the slope will increase and the edge will be sharpened. Now, for the given edge model, the rate that the slope changes will be studied. Then, the parameter k may be selected to maximize the edge sharpening effect of anisotropic diffusion.

For the 1-D continuous model, the diffusion coefficient for the edge (6) is

$$c_t(x) = \exp\left[\frac{-\frac{\partial}{\partial x}I_t(x)}{k^2}\right] = \exp\left[\frac{-Af\,\mathrm{sech}^2(fx+\theta)}{k^2}\right] \quad (9)$$

After computing $I_t''(x)$, $I_t'''(x)$, ϕ', and ϕ'', we obtain the rate of change of the slope using (8):

$$\frac{\partial}{\partial t}[I_t'(x)] = \exp\left[\frac{-Af\,\mathrm{sech}^2(fx+\theta)}{k^2}\right] \left[\begin{array}{l}\left(C_1C_2C_3C_4 - C_1C_2C_5 - C_1C_5 + C_1C_3C_6\right)\frac{1}{k^2} \\ +C_1C_2C_3C_5\frac{1}{k^4} - \left(C_1C_2C_4 + C_1C_6\right)\end{array}\right]. \quad (10)$$

The constants (w.r.t. k) in (10) are given by

$$C_1 = 4A^2f^5\,\mathrm{sech}^4(fx+\theta)\tanh(fx+\theta), \quad (11)$$

$$C_2 = 2Af^2\,\mathrm{sech}^4(fx+\theta)\tanh(fx+\theta), \quad (12)$$

$$C_3 = Af\,\mathrm{sech}^2(fx+\theta), \quad (13)$$

$$C_4 = 1-2\sinh^2(fx+\theta), \quad (14)$$

$$C_5 = 2Af\tanh^2(fx+\theta), \quad (15)$$

and

$$C_6 = 2\tanh^2(fx+\theta) - \mathrm{sech}^2(fx+\theta). \quad (16)$$

To examine how k affects the slope change, $\frac{\partial}{\partial k}\left\{\frac{\partial}{\partial t}[I_t'(x)]\right\}$ must be computed. From (10),

$$\frac{\partial}{\partial k}\left\{\frac{\partial}{\partial t}[I_t'(x)]\right\} = \frac{2}{k^3}\exp\left[\frac{-Af\,\mathrm{sech}^2(fx+\theta)}{k^2}\right] \left\{\begin{array}{l}\left(C_1C_2C_3C_4 - C_1C_2C_5 - C_1C_5 + C_1C_3C_6\right) \\ \left[\frac{Af}{k^2}\mathrm{sech}^2(fx+\theta) - 1\right] \\ +C_1C_2C_3C_5\frac{1}{k^2}\left[\frac{Af}{k^2}\mathrm{sech}^2(fx+\theta) - 2\right] \\ -\left(C_1C_2C_4 + C_1C_6\right)Af\,\mathrm{sech}^2(fx+\theta)\end{array}\right\} \quad (17)$$

Fig. 2 shows $\frac{\partial}{\partial t}[I_t'(x)]$ for several values of k, given the edge shown in Fig. 1. In this graph, the slope is observed in the neighborhood of the inflection point (at $x = 26$). One may note from the graph that increasing k beyond a certain point results in a negligible gain in edge enhancement (increase in slope). This limiting behavior is also obvious in Fig. 3, the graph of $\frac{\partial}{\partial k}\left\{\frac{\partial}{\partial t}[I_t'(x)]\right\}$. The form of $\frac{\partial}{\partial k}\left\{\frac{\partial}{\partial t}[I_t'(x)]\right\}$ may be used to determine k.

Let A represent the minimum contrast object that is desired for detection in the IR imagery. The slope of the edge at x_{ip} is Af, where f is selected according to the thermodynamic properties of the imaging environment (emissivity, background radiation, sensor characteristics). In the neighborhood of x_{ip}, use (17) to define k:

$$k = \min k:\ \frac{\partial}{\partial k}\left\{\frac{\partial}{\partial t}[I_t'(x)]\right\} < \varepsilon \text{ and } \frac{\partial}{\partial t}[I_t'(x)] > 0. \quad (18)$$

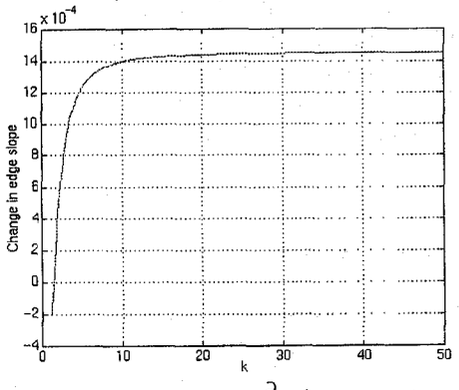

Fig. 2: Graph of $\frac{\partial}{\partial t}[I_t'(x)]$ vs. k for the edge shown in Fig. 1.

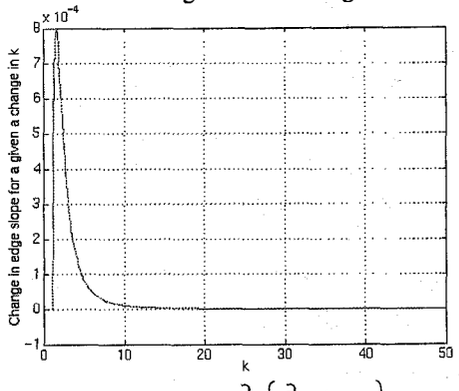

Fig. 3: Graph of $\frac{\partial}{\partial k}\left\{\frac{\partial}{\partial t}[I_t'(x)]\right\}$ vs. k for the edge shown in Fig. 1.

(18) suggests that the minimum k that produces the maximum sharpening is desired. Overspecification of k will lead to a loss of structure in the image. Because $\frac{\partial}{\partial t}[I_t'(x)]$ approaches 0 in the limit, but never equals 0, an ε-bound is applied. ε may be determined by the percentage of the maximum sharpening ability desired.

Since one of the goals of the pyramidal processing is to sharpen edges and avoid the "staircasing" artifacts of fixed-resolution diffusion, the root level R may be assigned by finding the lowest root level that guarantees step edges in the segmentation. In evaluating the level which leads to a piecewise constant segmentation of the IR image, the effects of sampling and anisotropic diffusion on the edge slope must be evaluated.

Given 1 of S sampling in each linear dimension, the effect of sampling on the edge slope is straightforward. Since the amplitude of the edge is not changed, and the width of the edge is modified by $1/S$, sampling will effectively increase the edge slope by a factor of S.

Now, let us examine the effect of anisotropic diffusion on the edge slope, for the discrete domain/range case. We can define the edge slope for any arbitrary edge as the edge magnitude divided by the distance between the points on the edge for which the edge is rising (or falling). Consider an edge that is rising from left to right and is governed by (6). The edge begins to rise after $x_{I_{\min}}$, where

$$x_{I_{\min}} = \max x : x < \frac{\tanh^{-1}\left(\frac{1-2A}{2A}\right)}{f} + x_{ip}, x \in \mathbf{Z}. \quad (19)$$

The point where the edge ceases to rise is at

$$x_{I_{\max}} = \min x : x > \frac{\tanh^{-1}\left(\frac{2A-1}{2A}\right)}{f} + x_{ip}, x \in \mathbf{Z}. \quad (20)$$

Combining (19) and (20), the effective slope before diffusion at level 0 is

$$m_0 = \frac{2A}{x_{I_{\max}} - x_{I_{\min}}} = \frac{Af}{\tanh^{-1}\left(\frac{2A-1}{2A}\right)}. \quad (21)$$

Now, the change in slope for the higher pyramid levels must be examined. In 1-D, the discrete anisotropic diffusion equation may be given as

$$I_{t+1}(x) = I_t(x) + (1/2)\left[c_{E,t}(x)\nabla I_{E,t}(x) + c_{W,t}(x)\nabla I_{W,t}(x)\right]. \quad (22)$$

Since, in the neighborhood of $x_{I_{\min}}$ and $x_{I_{\max}}$, $k^2 >> \nabla I_t^2(x)$, then $c_{E,t}(x) = c_{W,t}(x) \approx 1$. And by definition, there is no change in intensity one pixel to the left of $x_{I_{\min}}$ and one pixel to the right of $x_{I_{\max}}$. Likewise, there is a least a difference of one intensity level to the right of $x_{I_{\min}}$ and to the left of $x_{I_{\max}}$. Using (22) with the stated assumptions, the difference of $x_{I_{\max}} - x_{I_{\min}}$ decreases by at least a value of 1 and the slope thereby increases.

Considering the effects of sampling and diffusion together, the slope is modified with each ascending pyramid level as follows:

$$m_{l+1} \geq \frac{2AS}{\frac{2A}{m_l} - 1}. \quad (23)$$

If the slope becomes greater than or equal to $2A$, then the edge rises in one pixel, and step edges are obtained. So, R is selected by

$$R = \min l : m_l \geq 2A. \quad (24)$$

3. RESULTS AND CONCLUSIONS

The ADP edge-enhancing algorithm was applied to an IR video sequence of the space shuttle. The goal of this application was to first enhance and locate edges. Then, an edge-based template matching algorithm was used to determine the position of the target. For target tracking, the ADP yielded edge localization errors of under two pixels in each linear dimension. Fig. 4 shows an original IR image (intensity inverted) from the sequence with crosshairs giving the location of the space shuttle as computed by the ADP tracking program. Without the ADP segmentation process, an edge map with thick, spurious edges is generated as in Fig. 5. The ADP, however, generates well-localized, single pixel-width edges as shown in Fig. 6.

REFERENCES

[1] P.J. Burt, "Smart Sensing within a Pyramid Vision Machine," *Proceedings of the IEEE*, vol. 76, no. 8, pp. 1006-1015, Aug. 1988.

[2] S.T. Acton, A. C. Bovik, and M. M. Crawford, "Anisotropic Diffusion Pyramids for Image Segmentation," *Proceedings of the IEEE Int. Conference on Image Processing*, Austin, Texas, Nov. 1994.

[3] P. Perona and J. Malik, "Scale-Space and Edge Detection Using Anisotropic Diffusion," *IEEE Transactions on Pattern Analysis and Machine Intelligence*, vol. 12, no. 7, pp. 629-639, July 1990.

[4] Y. You, M. Kaveh, W. Xu, A. Tanenbaum, "Analysis and design of anisotropic diffusion for image processing," *Proceedings of the IEEE Int. Conference on Image Processing*, Austin, Texas, Nov. 1994.

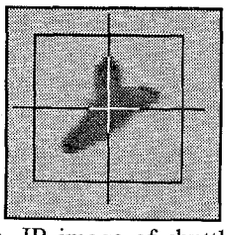

Fig. 4: IR image of shuttle with crosshairs marking the position as located by the ADP.

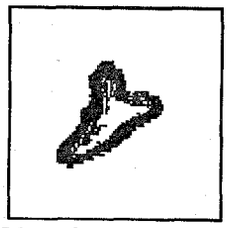

Fig. 5: Edges found in original image by thresholding the gradient magnitude.

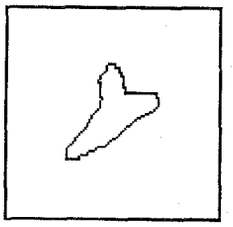

Fig. 6: Edges found after enhancement by the ADP.